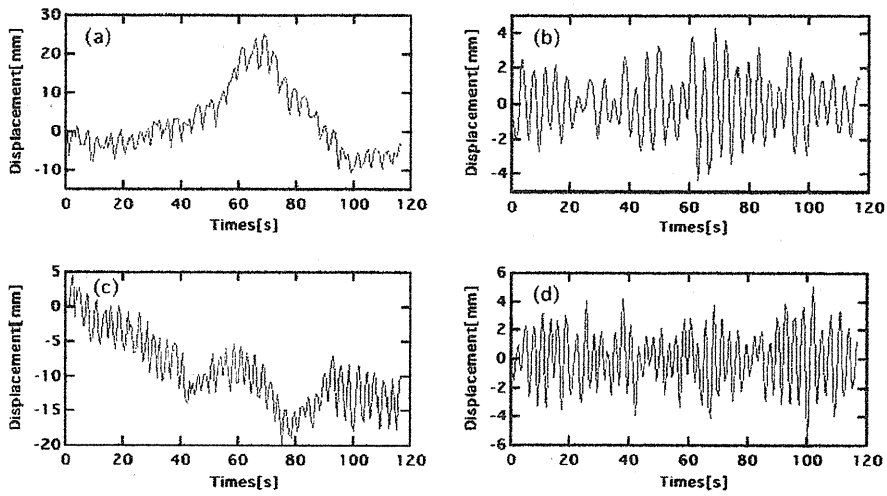


**Fig. 3.** Respiratory signal acquired by P-IBPR for patient 1 (a) before filtering and (b) after filtering and for patient 2 (c) before filtering and (d) after filtering.

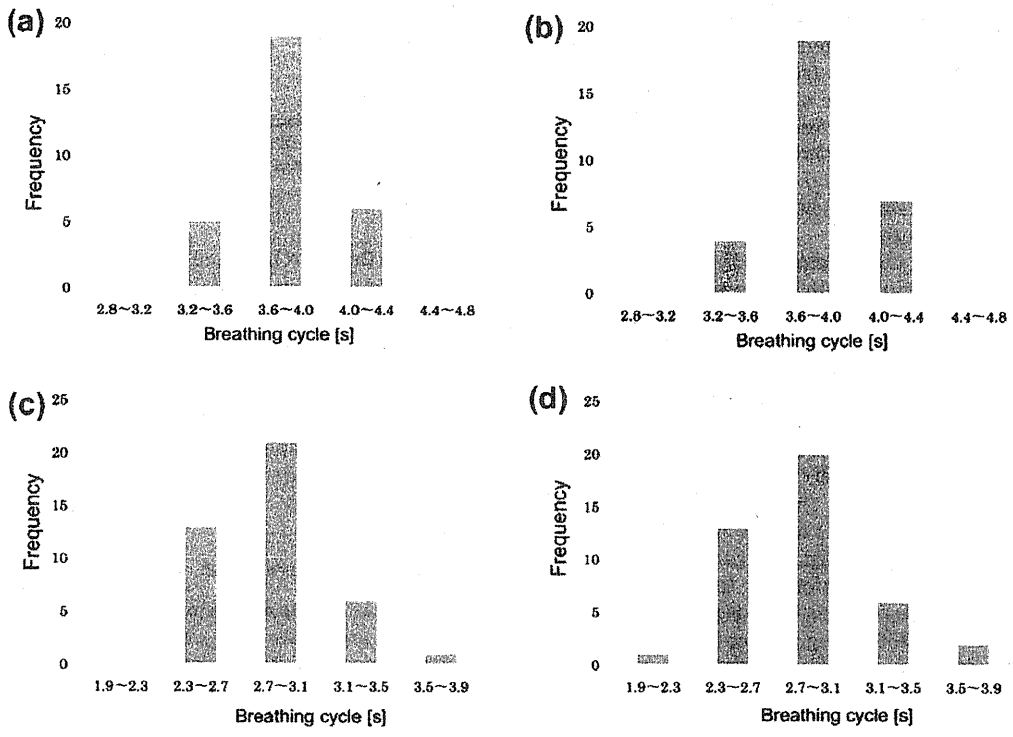


**Fig. 4.** Histograms of breathing cycle analysed by P-IBPR and visual tracking; (a) P-IBPR and (b) visual tracking for patient 1 and (c) P-IBPR and (d) visual tracking for patient 2.

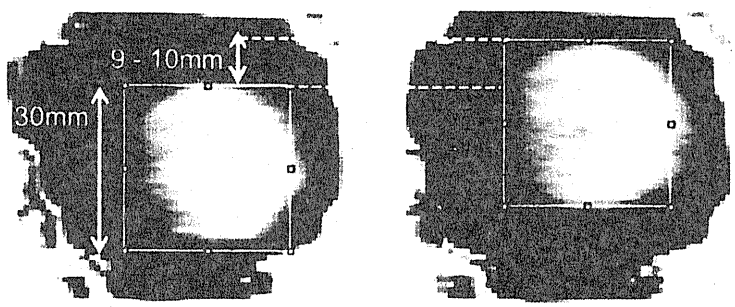


**Fig. 5.** Coronal images of 4D VMAT-CBCT of the QUASAR phantom in each peak. The diameter of the ball was 30 mm. The displacement was evaluated to be about 9–10 mm.

NAVIDIA Tesla C1060 4 GB. The amplitude was evaluated at about 9–10 mm from the 4D VMAT-CBCT images. This displacement is close to the mechanical set of 10 mm in the experiment. The inhomogeneous value inside the insert was observed.

*Reconstruction of 4D VMAT-CBCT in 2 patients*

With the respiratory signals acquired by P-IBPR, the portal images were classified into 4 phase bins. Then, VMAT-CBCT reconstruction was performed. For comparison, kV projection images were simultaneously acquired during VMAT, and 4D kV-CBCT was reconstructed. Fig. 6a and b illustrate the coronal and sagittal slices of VMAT-CBCT and kV-CBCT for 3D and the respiratory phases (max exhale, exhale inhale, max inhale, and inhale exhale) of patients 1 and 2.

The total number of portal images acquired during VMAT was 254 for both patients. Those images were almost equally classified into each phase bin. The gantry angle increment per projection for 4D reconstruction is dependent not only on the gantry speed but also on the respiratory cycle of the patient. These values for patients 1 and 2 were estimated as $5.4 \pm 0.8$ (1SD) and $3.9 \pm 0.5$ (1SD) degrees, respectively. Admittedly, there were large projection gaps that degraded image quality. In addition, this "effective" gantry angle increment included the error caused by the long acquisition interval of portal images, which was limited to 0.46 s per projection.

The centre of mass (COM) positions of the tumour during treatment were estimated from a contour of the tumour in respective max-exhale volume images in the Pinnacle treatment planning system and by shifting these contours in the other images. The shifts from the max exhale are denoted in Fig. 6. The results of 4D MV-CBCT were remarkably close to those of 4D kV-CBCT. The amplitudes of tumour motion during treatment for patients 1 and 2 were estimated to be about (1, 2, 5) and (2, 4, 5) mm, respectively. On the other hand, it was difficult to estimate tumour size due to diminished image quality and artifacts.

## Discussion

It should be noted that an exact and unique cone-beam reconstruction from portal images acquired in a VMAT delivery is impossible in principle [10]. That is, the VMAT-CBCT including our method is based on the assumption that there are few structures outside the radiation field. The effect of passing through objects outside the reconstructed region is naively considered by masking correction. However, as seen in Figs. 5 and 6 4D VMAT-CBCT showed the tumour position to be similar when predicted mechanically by the phantom and by the 4D kV-CBCT. We emphasise that we are interested in the visualisation of tumour motion for verification of actual treatment. From this viewpoint, we are satisfied that the amplitude can be evaluated from the 4D VMAT-CBCT images. Our method is, therefore, feasible for verifying tumour motion through the course of treatment. On the other hand, it should be noted that inconsistencies, such as the lack of projection data provided the degradation of image quality, and may lead to incorrect recognition for the tumour size and shape.

We employed the IBPR method using NCC to derive respiratory signals from portal images. Our experiments demonstrated that NCC can work well for frame-by-frame changes in irradiation intensity. Respiratory signals were readily obtained because the MLC speed was constrained by treatment planning optimisation. This constraint yielded field shapes similar to those created in conformal treatment. The fact that the tumour was located in the middle of the lung may explain why the MLC did not need to move drastically. Thus, a target was detected within a field through

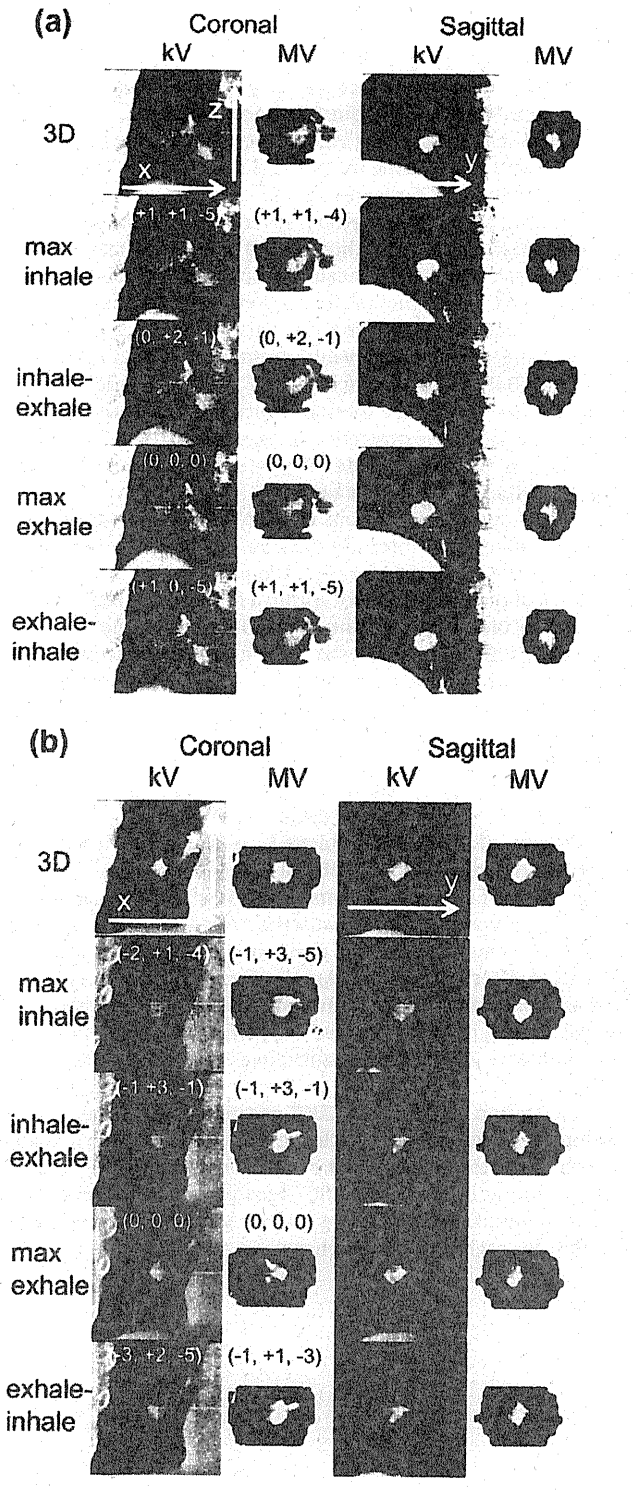


**Fig. 6.** Coronal and sagittal images at the isocentre plane of in-treatment kV 3D- and 4D-CBCT and 3D- and 4D-VMAT CT for (a) patient 1 and (b) patient 2. The coordinates inside the images represent the COM of tumour shift from max exhale with units in mm for each modality. The COMs were estimated from a contour delineated in respective max-exhale volume images on the Pinnacle treatment planning system and by shifting the contour in the other images.

almost all angles. On the other hand, the MLC constraint in the inverse plan may hinder clinical utility due to degradation of plan quality. In our clinical cases, this degradation was small and we judged that suppressing the MLC motion was beneficial for the

moving target. Of course, we cannot generalise our results, as this study was limited to 2 patients.

One of the advantages of IBPR is that no extra devices are required. It also provides direct tracking of tumour motion in contrast to methods that require external devices. In addition, correlations in the motion of inner structures and the body surface are not always measurable by external devices [15]. This is a critical problem for 4D-CT reconstruction.

In addition to our NCC method, several IBPR techniques such as the Amsterdam shroud method [11,12] and Kavanagh's method [13] have been proposed to acquire respiratory signals for kV projection images. The former projects 2D images onto the cranio-caudal axis to obtain a 1D signal for each image, while the latter utilises changes in the pixel value summation within each projection image. Both methods are based on pixel value projection and are easily affected by MLC motion, which yields drastic changes in pixel values within the projection images even if the MLC motion is as small as it was in our cases. Therefore, these methods would have difficulty with portal images.

Current issues or limitations of VMAT-CBCT reconstruction include the influence of intensity distribution and the shape yielded by MLC on the projection images. We performed a homogeneous correction of the total intensity within a field depending on the size and monitor unit. However, the change in field size yields an inhomogeneous intensity within the field, a matter that must be addressed in future studies. In addition, due to limitations of the Elekta iView software, the maximum number of portal imaging sequential acquisitions is only 256, so the acquisition of images may be insufficient for longer treatments. For stable P-IBPR, a sampling interval should be short enough to acquire a respiratory signal. Therefore, in this study, the shortest sampling rate of the Elekta iView software was employed, and the portal imaging was performed during less than half of a gantry rotation.

The inhomogeneous value inside the insert of the phantom as seen in Fig. 5 was also partly caused by this limitation. Optimised operation for the acquisition of portal images should be allowed in the system. Alternatively, a reconstruction algorithm can be developed as represented by digital tomosynthesis [16,17] and by compressed sensing [18] for a limited acquisition angle. The removal of such problems will enable quantitative derivation of 4D VMAT-CBCT.

In conclusion, a 4D VMAT-CBCT reconstruction technique was developed by using P-IBPR with the NCC method, which enabled us to obtain in-treatment volume images in 4 phases. The visibility of the anatomy in 4D VMAT-CBCT reconstruction for lung cancer patients makes this a promising tool for verifying relative tumour positions for each respiratory phase.

## Acknowledgements

This work was partially supported by JSPS KAKENHI 22791176. S.K. and A.H. wish to thank Dr. Grant Jackson (Elekta K.K.) for his advice regarding the use of iCom to acquire log data during treatment. K.N. received research funding from Elekta K.K.

## References

[1] van Elmpt W, McDermott L, Nijsten S, et al. A literature review of electronic portal imaging for radiotherapy dosimetry. Radiother Oncol 2008;88:289–309.
[2] Nijsten SM, Mijnheer BJ, Dekker AL, et al. Routine individualized patient dosimetry using electronic portal imaging devices. Radiother Oncol 2007;83:65–75.
[3] McDermott LN, Wendling M, Sonke JJ, et al. Replacing pretreatment verification with in vivo EPID dosimetry for prostate IMRT. Int J Radiat Oncol Biol Phys 2007;67:1568–77.
[4] Murphy MJ, Balter J, Balter S, et al. The management of imaging dose during image-guided radiotherapy: report of the AAPM Task Group 75. Med Phys 2007;34:4041–6063.
[5] Balter J, Benedict S, Bissonnette JP, et al. The role of in-room kV X-ray imaging for patient setup and target localization, AAPM Report No. 104. American Association of Physics in Medicine, 2009.
[6] Nakagawa K, Yamashita H, Shiraishi K, et al. Verification of in-treatment tumour position using kilovoltage cone-beam computed tomography: a preliminary study. Int J Radiat Oncol Biol Phys 2007;69:970–3.
[7] Nakagawa K, Haga A, Shiraishi K, et al. First clinical cone-beam CT imaging during volumetric modulated arc therapy. Radiother Oncol 2009;90:422–3.
[8] Ling C, Zhang P, Etmektzoglou T, et al. Acquisition of MV-scatter-free kilovoltage CBCT images during RapidArc™ or VMAT. Radiother Oncol 2011;100:145–9.
[9] Nakagawa K, Kida S, Haga A, et al. Cone beam computed tomography data acquisition during VMAT delivery with subsequent respiratory phase sorting based on projection image cross-correlation. J Radiat Res (Tokyo) 2011;52:112–3.
[10] Poludniowski G, Thomas MDR, Evans PM, et al. CT reconstruction from portal images acquired during volumetric-modulated arc therapy. Phys Med Biol 2011;55:5635–51.
[11] Sonke JJ, Zijp L, Remeijer P, van Herk M. Respiratory correlated cone beam CT. Med Phys 2005;32:1176–86.
[12] Zijp L, Sonke J, van Herk M. Extraction of the respiratory signal from sequential thorax cone-beam X-ray images. Jeong Publishing (Seoul) 2004:507–9.
[13] Kavanagh A, Evans PM, Hansen VN, et al. Obtaining breathing patterns from any sequential thoracic X-ray image set. Phys Med Biol 2009;54:4879–88.
[14] Otani Y, Fukuda I, Tsukamoto N, et al. A comparison of the respiratory signals acquired by different respiratory monitoring systems used in respiratory gated radiotherapy. Med Phys 2010;37:6178–86.
[15] Korreman SS, Juhler-Nottrup T, Boyer AL. Respiratory gated beam delivery cannot facilitate margin reduction, unless combined with respiratory correlated image guidance. Radiother Oncol 2008;86:61–8.
[16] Maurer J, Godfrey D, Wang Z, et al. On-board four-dimensional digital tomosynthesis: first experimental results. Med Phys 2008;35:3574–83.
[17] Maurer J, Pan T, Yin FF. Slow gantry rotation acquisition technique for on-board four-dimensional digital tomosynthesis. Med Phys 2010;37:921–33.
[18] Choi K, Wang J, Zhu L, et al. Compressed sensing based cone-beam computed tomography reconstruction with a first-order method. Med Phys 2010;37:5113–25.

*Acta Oncologica*, 2011; 50: 606–608

informa
healthcare

LETTER TO THE EDITOR

# Radiation therapy did not alleviate complete paralysis due to metastasis of lung adenocarcinoma to thoracic vertebrae until four months later

KEIICHI NAKAGAWA[1], KAE OHKUMA[1], HIDEOMI YAMASHITA[1], MAKOTO MASUDA[2], YUTAKA MATSUMOTO[2] & TAKAHIRO GOTOH[3]

[1]*Department of Radiology, University of Tokyo Hospital, Tokyo, Japan,* [2]*Department of Respirology, Yamato Municipal Hospital, Tokyo, Japan and* [3]*Department of Musculoskeletal Oncology, Tokyo Metropolitan Komagome Hospital, Tokyo, Japan*

**To the Editor,**

When malignant bone tumors metastasize into the spinal canal, the ensuing morbid sequelae includes not only pain but also paresthesia, weakness, and even complete paralysis. In such cases, because treatment delay by only two to three hours may cause permanent nerve injury, prompt treatment is necessary [1,2].

Since symptoms in association with paralysis impair the quality of life (QOL), surgery for decompression and the combined administration of steroids and radiation therapy may be selected [1,3,4]. In any case, once complete paralysis appears, recovery is difficult to achieve and active treatment may not be selected. Here we report a case in which difficulty in walking due to complete paralysis was alleviated by treatment and the ability to walk was not restored until four months later.

## Case report

On February 1, 2009, a 42-year-old male was admitted to the hospital with a chief complaint of lumbago of an unidentified cause. Although a manual muscle test of (MMT) grades 3–4 was recognized on admission, weakness in both lower limbs and difficulty in walking appeared on the same night and muscle strength weakened to MMT grades 1–2 on the next day (Table I).

(Subsequent descriptions of days of treatment and/or events are numbered from the day of admission, which was day one). Furthermore, on day 3, foot joints and the right large toe showed MMT grades 0 and 1, respectively, and other parts showed MMT grade 0. No paresthesia was recognized.

On day 5, numbness around the anus, incapable plantar flexion of the toe, and disappearance of voluntary movement of the anal sphincter appeared and all criteria for complete paralysis were satisfied. In terms of sensation, only incomplete paresthesia was observed, and numbness at the lower abdomen and the sense of touch on both lower limbs remained. Since bladder and rectal disturbance was detected and an urge to urinate and/or defecate was absent, a urethral catheter was inserted.

Computed tomography (CT) for exploration of the cause revealed a lung lesion (right upper lobe S3, 32 mm in diameter) and a metastatic bone lesion invading into the spinal canal at the tenth thoracic vertebra (Figure 1a and b). The metastatic lesion to the thoracic vertebra was osteoblastic and expanding to the vertebral body and the right transverse process. The swelling compressed the spinal cord from the ventral side, causing stenosis of the spinal canal.

CT-guided biopsy of the primary lesion led to the diagnosis of adenocarcinoma. CT showed no metastasis to lymph nodes but only the primary lesion and metastasis to the tenth thoracic spine. Non-small cell lung carcinoma (NSCLC) was diagnosed and staged as cT2N0M1 (bone metastasis) [5].

On day 5, palliative irradiation was started at 30 Gy/10 sessions/2 weeks to the metastatic lesion at the tenth thoracic spine. To prevent symptom aggravation due to edema by radiation therapy, dexamethasone

Correspondence: Hideomi Yamashita, Department of Radiology, University of Tokyo Hospital, 7-3-1, Hongo, Bunkyo-ku, Tokyo, 113-8655 Japan. Tel: + 81 3 5800 8667. Fax: + 81 3 5800 8935. E-mail: yamashitah-rad@h.u-tokyo.ac.jp

*(Received 7 November 2010; accepted 17 December 2010)*

ISSN 0284-186X print/ISSN 1651-226X online 
DOI: 10.3109/0284186X.2010.550314

Table I. On the admission day (day 1), the MMT grade was 3–4, but the MMT grade rapidly deteriorated bilaterally on the next day.

| | day 1 | | day 2 | |
|---|---|---|---|---|
| | R | L | R | L |
| SLR (straight leg raising test) | 80− | 60+ | | |
| FNS (femoral nerve stretching test) | − | − | | |
| Ilio psoas | 4 | 4 | 1–2 | 1–2 |
| Quadriceps | 4 | 3 | 3 | 3 |
| Tibialis anterior muscle | 4 | 3 | 1–2 | 1–2 |
| EHL (extensor hallucis longus) | 4 | 3 | 2 | 2 |
| FHL (flexor hallucis longus) | 4 | 4 | 2 | 2 |
| PTR (patellar tendon reflex) | + | + | | |
| ATR (Achilles tendon reflex) | + | ± | | |

8 mg/day was drip-infused from day 7 for nine days and at 4 mg/day thereafter for the remaining five days. For palliation of the pain by metastasis to the thoracic spine, oxycodone 10 mg/day was given from day 4 (on the day before beginning of radiation therapy) and the dose was gradually increased to 80 mg/day on day 20 with excellent pain control.

On day 24 (on day 20 after the beginning of radiation therapy), the pain was palliated and the dose was reduced. Since mutation in the epidermal growth factor receptor (EGFR) gene was confirmed, gefitinib was started on day 45 for systemic therapy. Another drug zoledronate was started on day 36 for palliation of bone-related events.

With the expectation of improving activities of daily life (ADL) by training of the upper limbs, rehabilitation to move to and from a wheelchair was started on week 3. On day 75 (55 days after the end of irradiation), there was reduction of abdominal and lumbar numbness and an urge to defecate appeared. Voluntary urination gradually became possible at four months. Furthermore, paralysis of the lower limbs was gradually alleviated during the same period and gradual but light movement of bilateral foot joints became possible, as well as the whole lower limbs below the knee joints.

Five months after admission, he was transferred to a rehabilitation hospital and rehabilitation was intensively started. He started training in a standing position and was able to walk with assistance or with a cane. Furthermore, he began to be able to urinate and to dress by himself albeit slowly.

One month later, he was able to walk in the room with a walker and/or a cane, and after two more months he was discharged from the hospital. Although needing to bear some weight on the cane, he began to be able to go up stairs.

Two months after discharge, he was able to walk without a cane. When he registered as a disabled person at the driving license center, the limitation of movement of his legs was mild, and he was judged to be able to drive a car without alterations.

Magnetic resonance imaging (MRI) eight months after radiation therapy revealed that the tenth thoracic vertebral body and bilateral transverse processes showed low signals by T1-weighted and T2-weighted images. This suggested osteoblastic bone metastasis, but there was almost no bone swelling or stenosis of the spinal canal. At the same level, the spinal cord was mildly atrophic and a T2-weighted image showed faintly high signals at the inner area (myelomalacia), which suggested that the spine had previously been under strong compression.

In addition, small bone metastatic lesions were found at the base of the spinous process of the 12th

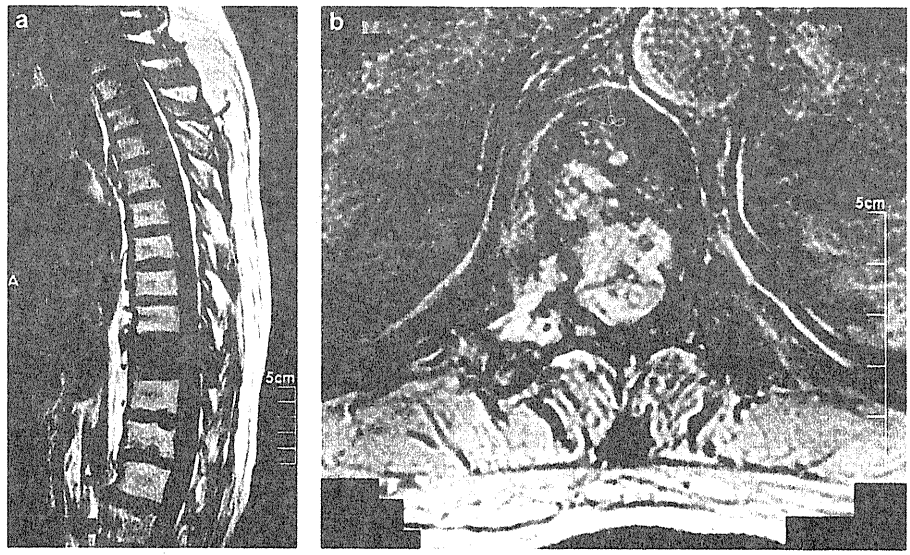


Figure 1. Osteoblastic metastatic bone tumor developing in the spinal canal at the tenth thoracic vertebra: (a), sagittal view; (b), horizontal view.

thoracic vertebra, but there was no evidence of stenosis of the spinal canal at other levels.

## Discussion

It is not rare for paralytic symptoms of the lower limbs due to metastatic vertebral tumors to be eliminated by treatment. To our knowledge, however, no case report described that laminectomy and/or radiation therapy enabled walking more than one week after autokinetic motion of the lower limbs became impossible due to metastases to the thoracic vertebrae.

Rades et al. devised a scoring system to report an improvement rate based on the period for appearance of paralytic symptoms due to metastasis to vertebrae, motor functions at the beginning of irradiation, presence or absence of other lesions, and the kind of the primary disease [6].

According to the scoring system, the status before treatment in the present case showed 24 points in total (primary disease, lung adenocarcinoma = 5 points; period after diagnosis, 15 months = 6 points; organ metastasis, absent = 8 points; motor function before irradiation, paraplegia = 1 point; and speed of aggravation of motor paralysis, 1–7 days = 4 points), and the improvement rate based on this score was 6%.

Radiation therapy was started on the day when complete paralysis appeared in the present case, and the symptom improvement rate was markedly low. In this case, gefitinib was administered for treatment in addition to radiation therapy to the metastatic lesions. The dose of irradiation was 30 Gy/10 fr which has been shown effective as a dose for palliative irradiation [7], but not as a curative dose.

The effect of radiation therapy is often observed a few weeks after treatment, but at the latest symptoms are generally alleviated before eight weeks after treatment. Symptomatic improvement was observed after a long period of two to six months after radiation therapy. When complete paralysis is not alleviated even one month after treatment, the clinical judgment is that more recovery is difficult. However, recovery after a longer period was observed in the present case. This was attributed to the reduction in tumor size by gefitinib in addition to the inhibition of tumor growth by radiation therapy. Nevertheless, such recovery is more likely to be attributable not only to the multimodality therapy but also to the active rehabilitation by the patient. It minimized muscle weakening and at least improved QOL. Furthermore, given the contribution to the improvement in general conditions, it might have the effect of prolonging the life of the patient.

When paralytic symptoms due to metastatic lesions are established, treatment may not be performed in some cases because recovery cannot achieved. However, we experienced a case in which recovery was observed several months after treatment. In addition, in this case intervention with active rehabilitation greatly contributed to improving ADL even when the prognosis was poor.

## References

[1] Newton HB. Neurologic complications of systemic cancer appears in Am Fam. Am Fam Physician 1999; 59: 878-886.
[2] Kvale PA, Simoff M, Prakash UB. American College of Chest Physicians. Lung cancer. Palliative care. Chest 2003; 123(suppl): S284-311.
[3] Brigden ML. Hematologic and oncologic emergencies. Doing the most good in the least time. Postgrad Med 2001; 109: 143-146, 151-154, 157-158.
[4] Rhodes V, Manzullo E. Oncologic emergencies. In: Pazdur R. Medical Oncology: A Comprehensive Review. 2nd ed. Huntington, N.Y.: PRR, 1997.
[5] UICC TNM Classification of Malignant Tumours, 6th edition.
[6] Dirk R, Volker R, Theo V, Lukas JAS, Hiba B, Johann HK, Peter JH, Steven ES. A Score Predictin g Posttreatment Ambulatory Status In Patients Irradiated For Metast atic Spinal Cord Compression. Int J Radiat Oncol Biol Phys 2009; 73: 228-234.
[7] Rades D, Lange M, Veninga T, Rudat V, Bajrovic A, Stalpers LJ, Dunst J, Schild SE. Preliminary results of spinal cord compression recurrence evaluation (score-1) study comparing short-course versus long-course radiotherapy for local control of malignant epidural spinal cord compression. Int J Radiat Oncol Biol Phys 2009; 73: 228-234.

# Technical Note: Extension of van Herk's treatment margin model for anisotropic systematic positioning errors in Cartesian coordinate system[a)]

Kiyoshi Yoda[b)]
*Elekta KK, 3-9-1 Shibaura, Minato-ku, Tokyo 108-0023, Japan*

Keiichi Nakagawa
*Department of Radiology, University of Tokyo Hospital 7-3-1 Hongo, Bunkyo-ku, Tokyo 113-8655, Japan*

(Received 11 April 2011; revised 6 May 2011; accepted for publication 10 May 2011; published 16 June 2011)

**Purpose:** A coefficient of a treatment margin model for anisotropic systematic positioning errors has been calculated in Cartesian coordinate system based on van Herk's analytical formulation.
**Methods:** Three-dimensional (3D) patient population distribution was formulated in Cartesian coordinate system to model anisotropic systematic positioning errors. Analytical 3D integration with anisotropic standard deviations $\Sigma$'s and the following Newton's method yielded the coefficient of van Herk's systematic positioning error model in Cartesian coordinate system.
**Results:** The treatment margins for the anisotropic systematic errors in Cartesian coordinate system were 2.1 $\Sigma$ for 90% patient population coverage and 2.4 $\Sigma$ for 95% patient population coverage.
**Conclusions:** It was found that the treatment margins for anisotropic systematic positioning errors in Cartesian coordinate system were smaller than those for the isotropic model in spherical coordinate system for a given patient population coverage probability. © *2011 American Association of Physicists in Medicine*. [DOI: 10.1118/1.3596531]

Key words: treatment margin, Cartesian coordinate system, systematic positioning errors

Marcel van Herk *et al.* proposed an analytical treatment margin model that considered both systematic positioning errors among all the patients in a facility and random positioning errors among all the treatment fractions for each patient.[1,2] The coefficients of the model parameters were numerically calculated under a spherically symmetric condition thereby leading to an isotropic margin perpendicular to a spherical tumor surface. However, recent high precision treatment is performed under Cartesian coordinate system with a 3 or 6 degrees-of-freedom couch, and the systematic positioning errors may be anisotropic. Although the original article mentioned an extension to anisotropic modeling,[1] detailed results have not been published.

In this article, three-dimensional (3D) Gaussian patient population is formulated in Cartesian coordinate system to model anisotropic systematic errors for patient positioning. Analytical integration with anisotropic standard deviations and the following Newton's method are performed to derive the coefficient of van Herk's systematic positioning error model in Cartesian coordinate system.

The 3D Gaussian patient population model is given by

$$G(x,\Sigma_x^2)G(y,\Sigma_y^2)G(z,\Sigma_z^2), \tag{1}$$

where $G(r,\Sigma_r^2)$ denotes the probability density of one-dimensional Gaussian distribution with a standard deviation of $\Sigma_r$, where r is x, y, or z. For example, $G(x,\Sigma_x^2)$ is given by

$$G(x,\Sigma_x^2) = \frac{e^{-\frac{x^2}{2\Sigma_x^2}}}{\sqrt{2\pi}\Sigma_x}. \tag{2}$$

The coverage probability of the patient population in the systematic positioning error ranges of $-c\,\Sigma_x < x < c\,\Sigma_x$, $-c\,\Sigma_y < y < c\,\Sigma_y$, and $-c\,\Sigma_z < z < c\,\Sigma_z$ is given by 3D integration of (1) leading to

$$\mathrm{erf}\left(\frac{c}{\sqrt{2}}\right)^3 \tag{3}$$

where c is an arbitrary positive constant, and erf is the error function. The analytical integration was performed by a computer code, Mathematica,[3] as shown in Fig. 1.

The expression (3) is a trivial form because it is the third power of the one-dimensional result shown in van Herk's paper,[1] however, to the author's knowledge it has not been calculated nor compared to the original van Herk's coefficient in spherical coordinate system. To solve the nonlinear equation, Newton's method was employed and the results are shown in Table I. Again, the numerical root finding was performed by Mathematica,[3] which is also shown in Fig. 1. It was found that the treatment margins for anisotropic systematic positioning errors in Cartesian coordinate system were smaller than those for the isotropic model in spherical coordinate system for a given patient population coverage probability.

In conclusion, van Herk's treatment margin model for systematic errors was reformulated by calculating the coefficient of the anisotropic systematic error model in Cartesian coordinate system. The resulting coefficient was smaller than that for the spherically symmetric model.

Further modification would be possible by integrating (1) with varied integration ranges in 3D directions. Meanwhile,

```
gaussian3Danisotropic =
  Function[{x, y, z},
        Exp[-x^2 / (2 sigmax^2)] / sigmax / Sqrt[2 Pi] *
        Exp[-y^2 / (2 sigmay^2)] / sigmay / Sqrt[2 Pi] *
        Exp[-z^2 / (2 sigmaz^2)] / sigmaz / Sqrt[2 Pi]
  ]
```

$$\text{Function}\left[\{x, y, z\}, \frac{e^{-\frac{x^2}{2\,\text{sigmax}^2}}\, e^{-\frac{y^2}{2\,\text{sigmay}^2}}\, e^{-\frac{z^2}{2\,\text{sigmaz}^2}}}{(\text{sigmax}\sqrt{2\pi})\,(\text{sigmay}\sqrt{2\pi})\,(\text{sigmaz}\sqrt{2\pi})}\right]$$

```
Integrate[
  gaussian3Danisotropic[x, y, z],
    {x, -Infinity, Infinity}, {y, -Infinity, Infinity}, {z, -Infinity, Infinity},
      Assumptions → {sigmax > 0, sigmay > 0, sigmaz > 0}
]

1

Integrate[
  gaussian3Danisotropic[x, y, z],
    {x, -c sigmax, c sigmax}, {y, -c sigmay, c sigmay}, {z, -c sigmaz, c sigmaz}
]
```

$$\text{Erf}\left[\frac{c}{\sqrt{2}}\right]^3$$

$$\text{FindRoot}\left[\text{erf}\left(\frac{c}{\sqrt{2}}\right)^3 = 0.8, \{c, 1.\}\right]$$

```
{c → 1.80113}
```

$$\text{FindRoot}\left[\text{erf}\left(\frac{c}{\sqrt{2}}\right)^3 = 0.85, \{c, 1.\}\right]$$

```
{c → 1.93711}
```

$$\text{FindRoot}\left[\text{erf}\left(\frac{c}{\sqrt{2}}\right)^3 = 0.9, \{c, 1.\}\right]$$

```
{c → 2.11405}
```

$$\text{FindRoot}\left[\text{erf}\left(\frac{c}{\sqrt{2}}\right)^3 = 0.95, \{c, 1.\}\right]$$

```
{c → 2.38774}
```

$$\text{FindRoot}\left[\text{erf}\left(\frac{c}{\sqrt{2}}\right)^3 = 0.99, \{c, 1.\}\right]$$

```
{c → 2.93416}
```

FIG. 1. A computer code for calculating the coefficient of van Herk's treatment margin model for anisotropic systematic positioning errors in Cartesian coordinate system. Each bold part is a command followed by each calculated result.

TABLE I. Treatment margins, $\alpha\,\Sigma$, for systematic positioning errors as a function of patient population coverage probability.

| Patient population coverage (%) | Cartesian 3D model ($\Sigma$) | Spherical 3D model ($\Sigma$) |
|---|---|---|
| 80 | 1.80 | 2.16 |
| 85 | 1.94 | 2.31 |
| 90 | 2.11 | 2.50 |
| 95 | 2.39 | 2.79 |
| 99 | 2.93 | 3.36 |

the present author believes that the most important point to keep in mind is that the present margin model excludes delineation errors in a clinical target volume.[1,2,4]

[a]Dr Nakagawa receives research funding from Elekta.
[b]Electronic mail: Kiyoshi.Yoda@elekta.com

[1]M. van Herk, P. Remeijer, C. Rasch, and J. V. Lebesque, "The probability of correct target dosage: Dose-population histograms for deriving treatment margins in radiotherapy," Int. J. Radiation Oncology Biol. Phys. **47**, 1121–1135 (2000).
[2]M. van Herk, "Errors and margins in radiotherapy," Semin. Radiat. Oncol. **14**, 52–64 (2004).
[3]S. Wolfram, *Mathematica, a System for Doing Mathematics by Computer* (Addison-Wesley, San Francisco, 1991).
[4]M. van Herk, "Will IGRT live up to its promise?," Acta Oncol. **47**, 1186–1187 (2008).

International Journal of
Radiation Oncology
biology • physics

www.redjournal.org

Clinical Investigation

# Integration of Corticospinal Tractography Reduces Motor Complications After Radiosurgery

**Tomoyuki Koga, M.D.,* Masahiro Shin, M.D.,* Keisuke Maruyama, M.D.,* Kyousuke Kamada, M.D.,* Takahiro Ota, M.D.,* Daisuke Itoh, M.D.,† Naoto Kunii, M.D.,* Kenji Ino, R.T.,† Shigeki Aoki, M.D.,† Yoshitaka Masutani, Ph.D.,† Hiroshi Igaki, M.D.,† Tsuyoshi Onoe, M.D.,† and Nobuhito Saito, M.D.***

*Departments of *Neurosurgery and †Radiology, The University of Tokyo Hospital, Tokyo, Japan*

Received Mar 25, 2011. Accepted for publication May 17, 2011

**Summary**

When diffusion-tensor tractography is integrated into stereotactic radiosurgery for brain arteriovenous malformations adverse events may be reduced although the effect on AVM obliteration rates is unknown. This study compared outcomes of patients treated with and without tractography. The integration of tractography of the corticospinal tract significantly reduced motor complication without compromising obliteration rate.

**Purpose:** To evaluate whether the use of diffusion-tensor tractography (DTT) of the corticospinal tract could reduce motor complications after stereotactic radiosurgery (SRS).
**Methods and Materials:** Patients with arteriovenous malformation (AVM) in the deep frontal lobe, deep parietal lobe, basal ganglia, and thalamus who had undergone radiosurgery since 2000 and were followed up for more than 3 years were studied. DTT of the corticospinal tract had been integrated into treatment planning of SRS since 2004, and the maximum dose received by the corticospinal tract was attempted to be less than 20 Gy. Treatment outcomes before (28 patients, Group A) and after (24 patients, Group B) the introduction of this technique were compared.
**Results:** There were no statistical differences between the two groups (Group A vs. Group B) in patients' age (34 years vs. 33 years, $p = 0.76$), percentage of patients with hemorrhagic events before treatment (50% vs. 29%, $p = 0.12$), or percentage of AVM involving the basal ganglia and thalamus (36% vs. 46%, $p = 0.46$). Obliteration rates were 69% and 76% at 4 years in Groups A and B, respectively ($p = 0.68$), which were not significantly different. Motor complications were observed in 5 patients in Group A (17.9%) but only in 1 patient in Group B (4.2%), which was significantly less frequent ($p = 0.021$).
**Conclusion:** Integrating DTT of the corticospinal tract into treatment planning contributed to reduction of motor complications without compromising the obliteration rate for AVM adjacent to the corticospinal tract. © 2011 Elsevier Inc.

**Keywords:** Arteriovenous malformation, Corticospinal tract, Diffusion-tensor tractography, Morbidity, Stereotactic radiosurgery

## Introduction

Stereotactic radiosurgery (SRS) is widely accepted as a treatment modality for brain disorders including brain neoplasms, vascular lesions, and functional disorders (1–5). Although SRS is known as one of the least invasive treatment modalities for cerebral arteriovenous malformations (AVM), the associated risk of radiation-induced neuropathy occurs in 5–20% of patients

Reprint requests to: Tomoyuki Koga, M.D., Department of Neurosurgery, The University of Tokyo Hospital, 7-3-1 Hongo, Bunkyo-ku, Tokyo 113-8655, Japan. Tel: (+81) 3-5800-8853; Fax: (+81) 3-5800-8655; E-mail: kouga-tky@umin.ac.jp

Conflict of interest: none.

Int J Radiation Oncol Biol Phys, Vol. ■, No. ■, pp. 1–5, 2011
0360-3016/$ - see front matter 
doi:10.1016/j.ijrobp.2011.05.036

(3, 6–9), which is not negligible for patients with AVM in deep-seated eloquent areas. To minimize such risk, we have integrated tractography of the brain white matter based on diffusion-tensor magnetic resonance imaging (MRI) into treatment planning of SRS using the Gamma Knife (10–12). Diffusion tensor tractography (DTT), one of the major recent advancements in MRI, enables clear visualization of various fibers inside the white matter of the brain that are not visible with conventional imaging methods (13). Until now, we have used this technology in SRS for more than 100 patients with AVM in the eloquent areas. However, it is still not clear whether modification of dose planning based on DTT has contributed to reduction of associated morbidity or how much the obliteration rate was affected by it. To clarify these issues, we analyzed the effect of integrating DTT of the corticospinal tract into treatment planning on neurologic complications and obliteration rates after SRS.

## Methods and Materials

### Patients

The data from patients with AVM in the deep frontal lobe, deep parietal lobe, basal ganglia, and thalamus were retrospectively analyzed because most of the lesions in these locations were considered to be close to the corticospinal tract and were classified as the eloquent area. After SRS, it usually takes 3 to 5 years to achieve radiographic obliteration of the treated AVM nidus (14). Thus, to evaluate obliteration rates, patients who were followed up for at least 3 years were included in this study.

We analyzed the outcomes in 52 patients with AVM in the deep frontal lobe, deep parietal lobe, basal ganglia, and thalamus after January 2000, in whom the same dose planning soft and imaging methods were used at SRS except for the use of DTT. Between January 2000 and January 2004, 28 patients were treated without the use of DTT (Group A). For these patients, after head fixation using a Leksell stereotactic frame, MRI and cerebral angiography were performed. Conformal treatment planning was made by the neurosurgeon and the radiation oncologist with the sophisticated software GammaPlan (15). All the patients in this group were treated by using a margin dose of 20 Gy or more. Since February 2004, we have begun to integrate DTT of the corticospinal tract, and 24 patients with those AVM were treated. Diffusion-tensor MRI was obtained on the day before treatment. Tractography was created from diffusion-tensor imaging by using freely shared programs, based on anatomic landmarks as shown in previous studies (10–13).

### Standard protocol approval, registration, and patient consent

The study was approved by the institutional review board at the University of Tokyo Hospital. Informed consent was obtained from all patients participating in the study.

### Procedures

On the day of treatment, patients were affixed to the stereotactic coordinate frame and underwent MRI and cerebral angiography. Then the MRI was registered by using the method as previously reported (10–12, 16). After the introduction of Gamma Knife 4C in October 2006, the registration process was automatized (17). Tractography-integrated images were imported to treatment planning software on the day of the treatment. Conformal treatment planning was made by experienced neurosurgeons and radiation oncologists by using treatment planning software GammaPlan. Radiotherapy of 15 to 20 Gy (median, 20 Gy) was given to the margin of the lesions by using 40–50% isodose lines, according to the volume of the nidus. The precise location of the corticospinal tract was confirmed on treatment planning images, and the maximum dose received by the corticospinal tract was restricted to be less than 20 Gy on the basis of previous analyses (Fig. 1) (10–12).

### Follow-up and statistical analysis

Serial formal neurologic and radiologic examinations were performed every 6 months after the procedure. The outcomes including motor complications, other adverse events, and complete obliteration confirmed by cerebral angiography were compared between Groups A and B. Statistical analyses were performed using JMP 8 (SAS Institute Inc., Cary, NC). Comparisons of patients' age, nidus volume, and follow-up period were performed by two-sample $t$ test. The rate of motor complications and other adverse events and the actuarial obliteration rate were calculated using the Kaplan-Meier method. The rates of adverse events and obliteration rates of patients in both groups were compared using the Cox proportional hazard model.

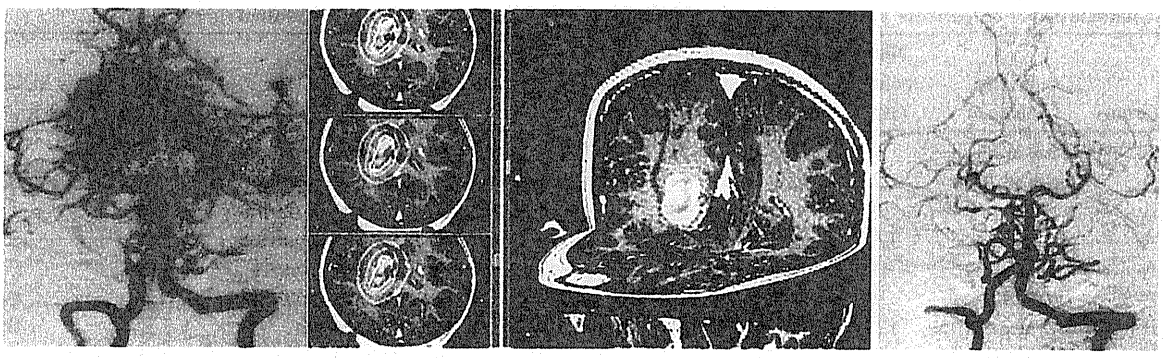

**Fig. 1.** Cerebral angiogram of a patient with right thalamic arteriovenous malformation (left). Treatment planning of radiosurgery with integration of diffusion-tensor tractography of the corticospinal tract (orange, middle). Cerebral angiogram taken at 36 months after treatment showed complete obliteration without any adverse event (right).

**Table 1** Comparison of characteristics of the patients in Groups A and B

| Characteristic | Group A | Group B | *p* value |
|---|---|---|---|
| Number of patients | 28 | 24 | – |
| Patient age (y) (mean, range) | 34, 8–64 | 33, 11–64 | 0.76 |
| Hemorrhage before treatment | 14 (50%) | 7 (29%) | 0.12 |
| Basal ganglia or thalamus | 10 (36%) | 11 (46%) | 0.46 |
| Treated volume ($cm^3$) (mean, range) | 4.8, 0.2–13.7 | 7.7, 1.1–22.4 | 0.026 |

## Results

### Comparison of the two groups

The patient characteristics and treatments in both groups are summarized in Table 1. There were no statistical difference between the two groups (Group A vs. Group B) in patients' age at treatment (34 years vs. 33 years, $p = 0.76$), percentage of patients with hemorrhagic events before treatment (50% vs. 29%), or percentage of AVM involving the basal ganglia and thalamus (36% vs. 46%, $p = 0.46$). The treated volume was significantly smaller ($p = 0{\cdot}026$) in Group A (mean, 4.8 $cm^3$; range, 0.2–13.7 $cm^3$) than in Group B (mean, 7.7 $cm^3$; range, 1.1–22.4 $cm^3$), and the applied marginal dose was lower in Group B (mean, 19.6 Gy; range, 15–20 Gy) than in Group A (mean, 20.2 Gy; range, 20–25 Gy). The median follow-up period was 62 months (range, 36–113 months) in Group A and 48 months (range, 36–80 months) in Group B ($p = 0.004$).

**Table 2** Factors associated with angiographically confirmed obliteration of the arteriovenous malformation nidus after stereotactic radiosurgery

| Factor | *p* value |
|---|---|
| Group A | 0.70 |
| Younger patient age | 0.13 |
| Hemorrhage before treatment | 0.49 |
| Location other than the basal ganglia and thalamus | 0.12 |
| Smaller treated volume | 0.42 |

### Nidus obliteration

Angiographically confirmed nidus obliteration rates at 4 years after SRS was 69% in Group A and 76% in Group B. Integration of DTT was not significantly associated with obliteration rate ($p = 0.68$) (Table 2). Latency interval hemorrhage after treatment occurred in 1 patient, in whom no worsening of neurologic symptom was observed.

### Complications

During the follow-up period, neurologic events occurred in 9 patients, 6 in Group A and 3 in Group B (Table 3). In Group A, transient hemiparesis was observed in 3 patients, permanent hemiparesis in 1, permanent dysesthesia in 1, and both permanent hemiparesis and dysesthesia in 1 patient. Modified Rankin Scale scores at last follow-up in these 6 patients were 0 in 3 patients, 1 in 1 patient, and 2 in 2 patients. In Group B, transient hemiparesis, permanent dysesthesia, and transient motor aphasia were observed in 1 patient each. Modified Rankin Scale scores at the last follow-up in these 4 patients were 0 in 3 patients and 1 in 1 patient. Deterioration of modified Rankin Scale scores at the last follow-up was observed in 3 patients among the 6 patients in Group A and 1 patient among 3 patients in Group B.

When we analyzed factors associated with the risk of neurologic events after SRS, integration of DTT of the corticospinal tract did not significantly ameliorate the overall risks of any kind of morbidity ($p = 0.18$), and involvement of the basal ganglia or thalamus was solely associated with higher risks ($p = 0.007$) (Table 4).

However, focusing on motor complications, Group A or the use of DTT of the corticospinal tract was significantly associated with

**Table 3** Characteristics of patients who experienced neurologic deterioration after stereotactic radiosurgery

| Age/sex | Group | Nidus location | Nidus volume ($cm^3$) | Margin dose (Gy) | Timing of obliteration (mo) | Follow-up period (mo) | Kind of morbidity | Timing of morbidity (mo) | MRS at last follow-up |
|---|---|---|---|---|---|---|---|---|---|
| 26/F | A | Thalamus | 9.2 | 20 | 35 | 60 | Hemiparesis/dysesthesia | 4 | 2 |
| 64/M | A | Frontal lobe | 2.0 | 20 | ND | 46 | Transient hemiparesis | 11 | 0 |
| 24/M | A | Thalamus | 2.5 | 20 | 36 | 39 | Permanent dysesthesia | 1 | 1 |
| 11/M | A | Thalamus | 12.3 | 20 | 39 | 87 | Permanent hemiparesis | 11 | 2 |
| 20/F | A | Basal ganglia | 0.4 | 20 | 38 | 38 | Transient hemiparesis | 16 | 0 |
| 28/M | A | Frontal lobe | 8.5 | 20 | 36 | 36 | Transient hemiparesis | 16 | 0 |
| 48/M | B | Basal ganglia | 12.9 | 20 | 44 | 63 | Transient aphasia | 2 | 0 |
| 14/F | B | Thalamus | 5.3 | 20 | 46 | 46 | Permanent dysesthesia | 10 | 1 |
| 25/F | B | Basal ganglia | 13.0 | 18 | 24 | 36 | Transient hemiparesis | 11 | 0 |

*Abbreviations:* MRS = modified Rankin Score; ND = data not available.

**Table 4** Factors associated with any kind of morbidity after stereotactic radiosurgery

| Factor | $p$ value |
|---|---|
| Group A | 0.18 |
| Older patient age | 0.33 |
| Larger treated volume | 0.17 |
| Involvement of the basal ganglia or thalamus | 0.007 |

**Table 5** Factors associated with motor complications after stereotactic radiosurgery

| Factor | $p$ value |
|---|---|
| Group A | 0.021 |
| Older patient age | 0.71 |
| Larger treated volume | 0.091 |
| Involvement of the basal ganglia or thalamus | 0.065 |

a lower rate of motor complications ($p = 0.021$) (Table 5). Namely, it indicated that SRS using DTT of the corticospinal tract at dose planning could significantly reduce those risks (5 patients in Group A vs. 1 in Group B).

In the patient who had transient hemiparesis in Group B, the volume of AVM nidus that was located in the basal ganglia was relatively large: 13.0 $cm^3$. The lesion was treated with a margin dose of 18 Gy, and the maximum dose delivered to the corticospinal tract was 17 Gy (Fig. 2).

## Discussion

Since the introduction of DTT-integrated SRS, we have partially modified treatment dose planning at SRS for AVM (10–12, 16) to restrict the irradiation dose to the adjacent motor fibers, and our early data suggested that SRS with integration of DTT was likely to be useful to prevent radiation-induced adverse events in AVM patients (10, 11, 18). With the accumulation of cases and the follow-up in this study, we evaluated the substantial effects of this technique because two principal concerns still remained unknown: whether integration of DTT could actually eliminate the risk of radiation-induced motor complications in any AVM patients, and how much such dose modifications would affect the other therapeutic effects such as nidus obliteration rates. Our results showed that SRS with DTT of the corticospinal tract could significantly reduce associated radiation-induced motor complications without affecting the nidus obliteration rates, proving that it contributes to preventing one of the most undesirable complications of SRS for AVM.

However,1 patient had a large nidus involving the basal ganglia and experienced transient hemiparesis after DTT-integrated SRS, which raised another issue. In this patient, the maximum dose received by the corticospinal tract was less than 20 Gy, which had been considered as a tolerable dose to the motor fibers in our preliminary results (10, 11). Larger nidus volume might have exposed the larger portion of the corticospinal tract to a relatively high dose even though the maximum dose did not surpass the tolerable dose, and this might have caused the hemiparesis. Also, the motor fibers passing through the internal capsule, close to the basal ganglia, are assembled in relatively small territories and are more likely to be affected than are fibers close to the cortical areas (10). Therefore, we speculate that the maximum dose to the corticospinal tract is not the only factor in the development of motor complications after SRS, but the extent of irradiated volume of the motor fibers and the irradiated part can be also associated with them as previously analyzed (10).

DTT has been widely used, and its usefulness has been established especially as a diagnostic tool (19). However, the major concern with regard to tractography is its reliability. If the tracts are not shown on the image, that does not always mean that the fibers do not exist (19, 20). By contrast, it has been shown by intraoperative fiber stimulation analysis that the tracts seen on DTT reflect the functioning white matter fibers to some extent (21).

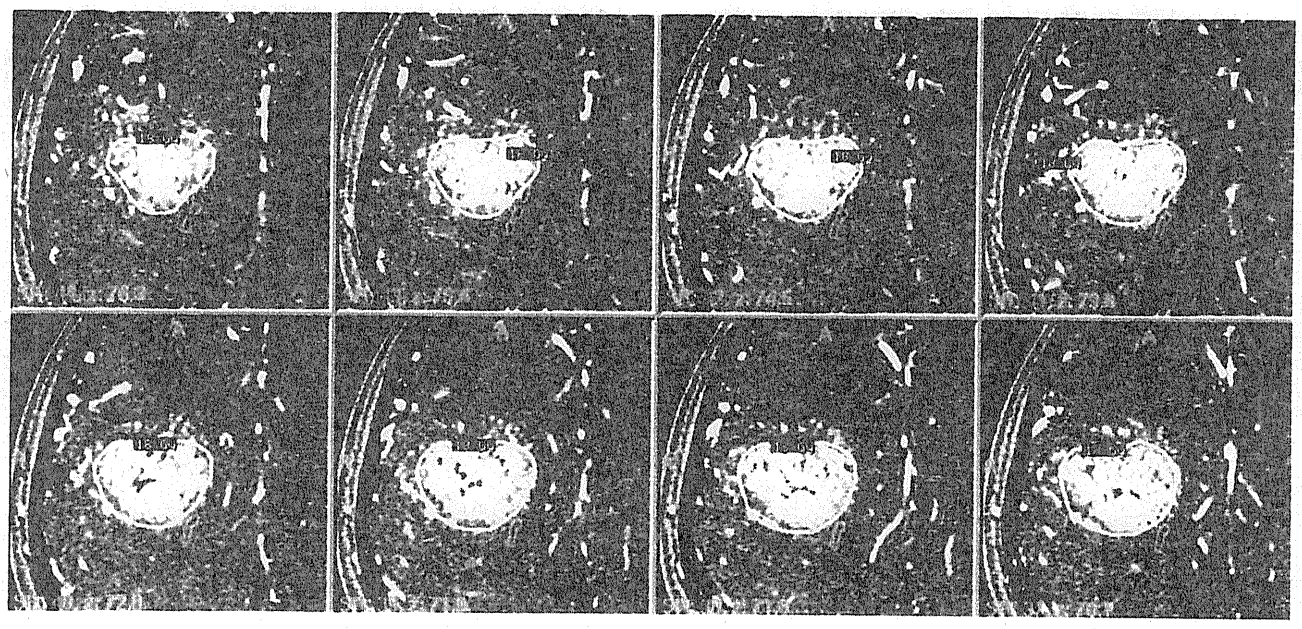

**Fig. 2.** Treatment planning for a patient with right frontal arteriovenous malformation who experienced transient left hemiparesis after radiosurgery. Long portion of the corticospinal tract (orange) was located adjacent to the large nidus.

Furthermore, those imaging methods are suitable for SRS because SRS has no risk of brain shift caused by craniotomy or tumor removal, which is inevitable in intraoperative applications (22).

The obliteration rates in the cohort in this study, which were 69–76 % at 4 years, were relatively low compared with those previously published (14). Inasmuch as it has been reported that obliteration rates of deeply located AVM have been low, 57–74% within 3 to 4 years (8, 23, 24), and that the lesions in 36–46% of the patients in this study were deeply located AVM, the lower obliteration rates might be explained by patient selection.

Further accumulation of cases with longer follow-up data is awaited to evaluate the effect of integrating tractography into Gamma Knife SRS, but our study disclosed that integrating DTT of the corticospinal tract into treatment planning at SRS contributed to reduction of motor complications and achieved safer treatment without compromising the obliteration rate for AVM adjacent to motor fibers.

## References


1. Koga T, Shin M, Saito N. Role of gamma knife radiosurgery in neurosurgery: Past and future perspectives. *Neurol Med Chir (Tokyo)* 2010;50:737–748.
2. Leksell L. Cerebral radiosurgery. I. Gammathalamotomy in two cases of intractable pain. *Acta Chir Scand* 1968;134:585–595.
3. Maruyama K, Kawahara N, Shin M, *et al.* The risk of hemorrhage after radiosurgery for cerebral arteriovenous malformations. *N Engl J Med* 2005;352:146–153.
4. Maruyama K, Kondziolka D, Niranjan A, *et al.* Stereotactic radiosurgery for brainstem arteriovenous malformations: Factors affecting outcome. *J Neurosurg* 2004;100:407–413.
5. Maruyama K, Shin M, Kurita H, *et al.* Proposed treatment strategy for cavernous sinus meningiomas: A prospective study. *Neurosurgery* 2004;55:1068–1075.
6. Andrade-Souza YM, Zadeh G, Scora D, *et al.* Radiosurgery for basal ganglia, internal capsule, and thalamus arteriovenous malformation: Clinical outcome. *Neurosurgery* 2005;56:56–64.
7. Flickinger JC, Kondziolka D, Lunsford LD, *et al.* A multi-institutional analysis of complication outcomes after arteriovenous malformation radiosurgery. *Int J Radiat Oncol Biol Phys* 1999;44:67–74.
8. Pollock BE, Gorman DA, Brown PD. Radiosurgery for arteriovenous malformations of the basal ganglia, thalamus, and brainstem. *J Neurosurg* 2004;100:210–214.
9. Sasaki T, Kurita H, Saito I, *et al.* Arteriovenous malformations in the basal ganglia and thalamus: Management and results in 101 cases. *J Neurosurg* 1998;88:285–292.
10. Maruyama K, Kamada K, Ota T, *et al.* Tolerance of pyramidal tract to gamma knife radiosurgery based on diffusion-tensor tractography. *Int J Radiat Oncol Biol Phys* 2008;70:1330–1335.
11. Maruyama K, Kamada K, Shin M, *et al.* Integration of three-dimensional corticospinal tractography into treatment planning for gamma knife surgery. *J Neurosurg* 2005;102:673–677.
12. Maruyama K, Kamada K, Shin M, *et al.* Optic radiation tractography integrated into simulated treatment planning for Gamma Knife surgery. *J Neurosurg* 2007;107:721–726.
13. Masutani Y, Aoki S, Abe O, *et al.* MR diffusion tensor imaging: Recent advance and new techniques for diffusion tensor visualization. *Eur J Radiol* 2003;46:53–66.
14. Shin M, Maruyama K, Kurita H, *et al.* Analysis of nidus obliteration rates after gamma knife surgery for arteriovenous malformations based on long-term follow-up data: The University of Tokyo experience. *J Neurosurg* 2004;101:18–24.
15. Koga T, Shin M, Maruyama K, *et al.* Long-term outcomes of stereotactic radiosurgery for arteriovenous malformations in the thalamus. *Neurosurgery* 2010;67:398–403.
16. Maruyama K, Koga T, Kamada K, *et al.* Arcuate fasciculus tractography integrated into Gamma Knife surgery. *J Neurosurg* 2009;111:520–526.
17. Koga T, Maruyama K, Igaki H, *et al.* The value of image coregistration during stereotactic radiosurgery. *Acta Neurochir (Wien)* 2009;151:465–471. discussion 471.
18. Koga T, Maruyama K, Kamada K, *et al.* Outcomes of diffusion tensor tractography-integrated stereotactic radiosurgery. *Int J Radiat Oncol Biol Phys*, In press.
19. Yamada K, Sakai K, Akazawa K, *et al.* MR tractography: A review of its clinical applications. *Magn Reson Med Sci* 2009;8:165–174.
20. Holodny AI, Watts R, Korneinko VN, *et al.* Diffusion tensor tractography of the motor white matter tracts in man: Current controversies and future directions. *Ann N Y Acad Sci* 2005;1064:88–97.
21. Kamada K, Todo T, Ota T, *et al.* The motor-evoked potential threshold evaluated by tractography and electrical stimulation. *J Neurosurg* 2009;111:785–795.
22. Kamada K, Todo T, Masutani Y, *et al.* Combined use of tractography-integrated functional neuronavigation and direct fiber stimulation. *J Neurosurg* 2005;102:664–672.
23. Kiran NA, Kale SS, Kasliwal MK, *et al.* Gamma knife radiosurgery for arteriovenous malformations of basal ganglia, thalamus and brainstem: A retrospective study comparing the results with that for AVMs at other intracranial locations. *Acta Neurochir (Wien)* 2009;151:1575–1582.
24. Andrade-Souza YM, Zadeh G, Scora D, *et al.* Radiosurgery for basal ganglia, internal capsule, and thalamus arteriovenous malformation: Clinical outcome. *Neurosurgery* 2005;56:56–63. discussion 63–54.

Int J Colorectal Dis (2011) 26:911–917
DOI 10.1007/s00384-011-1156-1

ORIGINAL ARTICLE

# Prognostic significance of adverse events associated with preoperative radiotherapy for rectal cancer

**Soichiro Ishihara · Toshiaki Watanabe · Takuya Akahane · Ryu Shimada · Atsushi Horiuchi · Hajima Shibuya · Tamuro Hayama · Hideki Yamada · Keijiro Nozawa · Hiroshi Igaki · Keiji Matsuda**

Accepted: 1 February 2011 / Published online: 22 February 2011


**Abstract**
*Purpose* Adverse events may occur in patients receiving preoperative radiotherapy (PRT) for rectal cancers. The aim of this study is to clarify the clinical and pathological features of the patients with PRT-related adverse events, and the significance of the adverse events on the clinical outcome.
*Methods* Seventy-five patients with T3 or T4 low rectal cancers curatively resected following PRT were studied. Thirty-one patients received radiotherapy, and 44 patients received chemoradiotherapy with tegafur-uracil and leucovorin. The total radiation dose was 50–50.4 Gy given in 25–28 fractions and the operation was performed 4–8 weeks after PRT. PRT-related adverse events were graded in accordance with the Common Terminology Criteria for Adverse Events v3.0.
*Results* The most frequent adverse events were leukocytopenia and diarrhea, observed in 12% and 24% of patients, respectively. The majority of the leukocytopenia and diarrhea was grade 1–2 toxicity. Women experienced leukocytopenia more frequently than men (28% vs. 7%, $p$=0.0317); however, no other predisposing factor for adverse events was recognized. Patients with leukocytopenia or diarrhea showed a better 5-year relapse-free survival rate than those without (94±5% vs. 49±9%, $p$=0.00054), and the presence of these adverse events was an independent prognostic factor in a multivariate analysis.
*Conclusions* The presence of leukocytopenia or diarrhea was an independent predictor of a fair prognosis after curative operation following PRT, and thus these adverse events seem not to discourage oncologists and patients from considering PRT for rectal cancers.

**Keywords** Rectal cancer · Radiotherapy · Chemotherapy · Adverse events · Surgery

S. Ishihara (✉) · T. Watanabe · T. Akahane · R. Shimada · A. Horiuchi · H. Shibuya · T. Hayama · H. Yamada · K. Nozawa · K. Matsuda
Department of Surgery, Teikyo University,
2-11-1, Kaga,
Itabashi-ku, Tokyo 173-8605, Japan
e-mail: sochan31@hotmail.com

H. Igaki
Department of Radiology, Teikyo University,
2-11-1, Kaga,
Itabashi-ku, Tokyo 173-8605, Japan

## Introduction

Preoperative radiotherapy for rectal cancer (PRT) has been shown to reduce postoperative locoregional recurrence, and, although controversial, is suggested to possibly improve postoperative survival of the patients [1–4]. Thus, PRT has now become widely accepted in modern surgical practice of rectal cancer. In spite of such clinical benefit, some patients experience adverse events associated with PRT or concomitantly administered chemotherapy, such as leukocytopenia and diarrhea. Likewise, the therapeutic effectiveness of PRT differs among patients, the degree of toxicity of PRT largely differs; some patients experiencing almost no adverse event and others experiencing relatively severe ones, although discontinuation of the neoadjuvant therapy is rarely necessary [5–7]. However, predisposing individual patient factors and the clinical significance of the PRT-related adverse events are not clear. Therefore, we aimed to clarify the clinical and pathological features of patients who suffer from adverse events following PRT, and the significance of the adverse events on the clinical outcome.

## Materials and methods

### Patients

Consecutive 85 patients with T3–T4 and M0 low rectal cancer (lying below the peritoneal reflection) received PRT at Teikyo University Hospital between February 1997 and July 2009. Preoperative staging was performed by digital examination, colonoscopy, endorectal ultrasound, barium enema, and computed tomography (CT). In recent cases, magnetic resonance imaging (MRI) was also employed, and positron emission tomography (PET) was done when necessary. Ten patients resulted in non-curative resection (positive circumferential margin in five patients, presence of distant metastasis in six patients) and were excluded from analysis. Thus, 75 patients comprised the study population. The patients were checked for PRT-related adverse events at least once a week and their severity was graded in accordance with the Common Terminology Criteria for Adverse Events (CTCAE) v3.0 (National Cancer Institute).

### Radiation methods and chemotherapy regimen

All the patients received pelvic preoperative radiotherapy as we have described previously [8], and briefly as follows. The total dose of preoperative radiotherapy was 50 Gy or 50.4 Gy, which was given in a fractionated manner over a long time period (2 Gy×25 Fr over 5 weeks or 1.8 Gy× 28 Fr over 6 weeks, respectively) in the supine position. Treatment planning was done using CT scans so that the clinical target volume included the primary tumor, anus, and regional lymph nodes. The regional lymph nodes included nodes around the inferior mesenteric, internal iliac, and middle rectal vessels; the presacral nodes; and the nodes around the obturator foramen. The planning target volume was defined in several planes. Cranially, the limit was defined at the level of superior margin of L5. Caudally, the limit was defined at the level of inferior margin of the ischial bone. This corresponded to the level of 1 cm below the anal orifice. The lateral limit was defined as 2 cm outside the bony pelvis. Dorsally, the whole sacrum and coccyx were included. Ventrally, the external iliac artery was excluded from the planning target volume. Forty-four patients received tegafur-uracil (300–500 mg/day) and leucovorin (75 mg/day) with radiotherapy.

### Surgical method

Four to 8 weeks after the completion of preoperative radiotherapy, a curative-intent operation was performed. Cases of non-curative resection were excluded from this study. The surgical procedures consisted of a low anterior resection, abdominoperineal resection, the Hartmann operation, and total pelvic exenteration. All procedures included lymphadenectomy using a standard total mesorectal excision (TME) technique with dissection of the perirectal lymph nodes and lymph nodes along the superior rectal artery. Lateral pelvic nodes were dissected in selected cases with suspicion of lateral node involvement prior treatment. Patients were surveyed for recurrence after surgery by CEA level (every 3 months), CT scan (every 6 months), and colonoscopy (every 12 months). Two patients were lost to follow-up, and the mean follow-up period was 37.1 months.

### Pathological study

All the resected specimens were examined pathologically, and the findings were recorded in accordance with the TNM classification [9]. In addition to routine pathological findings, the histological regression of the primary rectal lesion in response to PRT was evaluated and classified as high or low, based on the amount of residual cancer according to the classification of the Japanese Society for Cancer of the Colon and Rectum [10]. Cases in which more than two thirds of the cancer had degraded, necrotized, or disappeared were classified as high histological regression (including cases with a pathological complete response), and those in which less than two thirds of the cancer had degraded, necrotized, or disappeared were classified as low regression. Tumor downsizing in response to PRT was evaluated by the ratio of the tumor size in the resected specimen to the tumor size prior to PRT measured by barium enema. The cut-off value for the size ratio was 0.6, which was the median of the study population.

### Statistical analysis

Relapse-free survival curves were created using the Kaplan–Meier method and were compared using the log-rank test. Recurrence or metastasis of rectal cancer and death by any cause were counted as events. A multivariate analysis for factors associated with relapse-free survival was performed using the Cox proportional hazard model. A paired $t$ test, chi-square test, and Fisher's exact test were also performed where indicated. A $p$ value less than 0.05 was considered to denote statistical significance.

## Results

The major adverse events of PRT were leukocytopenia and diarrhea, and they were observed in nine (12%) and 18 (24%) patients, respectively. The majority of the leukocytopenia and diarrhea was grade 1–2, and only one patient experienced grade 3 diarrhea (Table 1). Other adverse events included appetite loss (grade 2 in two patients), eruption (grade 2 in

**Table 1** Severity of leukocytopenia and diarrhea

| | Grade 1 | Grade 2 | Grade 3 |
|---|---|---|---|
| Leukocytopenia | 6 (8%) | 3 (4%) | 0 |
| Diarrhea | 10 (13%) | 7 (9%) | 1 (1%) |

one patient), and thrombocytopenia (grade 1 in six patients), all of which were grade 1–2. Some degree of radiation dermatitis was almost inevitable, and was grade 1–2 except for grade 3 in one patient. No grade 4–5 adverse events were observed. Dose reduction or discontinuation of chemotherapeutic agents was necessary in three patients, and radiotherapy was completed as scheduled in all the patients. All the adverse events were resolved before the operations, and the operations were performed as planned in all the patients.

We compared the clinical and pathological features of the patients with leukocytopenia or diarrhea, the major adverse events of PRT, and those without (Table 2). Half of the female patients experienced leukocytopenia or diarrhea in comparison to 26% of the male patients, although the difference was not statistically significant. When each of these adverse events was analyzed separately, leukocytopenia was observed significantly more frequently in female patients than male patients (28% vs. 7%, $p$=0.0317); however, no gender difference was apparent in diarrhea. In patients with these adverse events, there seems to be a tendency that histological regression or downsizing of the

**Table 2** Clinical and pathological features of patients with adverse events

| | Leukocytopenia/diarrhea | | | Leukocytopenia | | | Diarrhea | | |
|---|---|---|---|---|---|---|---|---|---|
| | + ($n$=24) | − ($n$=51) | $p$ value | + ($n$=9) | − ($n$=66) | $p$ value | + ($n$=18) | − ($n$=57) | $p$ value |
| Sex | | | | | | | | | |
| Male | 15 | 42 | 0.0604 | 4 | 53 | **0.0317** | 12 | 45 | 0.2875 |
| Female | 9 | 9 | | 5 | 13 | | 6 | 12 | |
| Age (years) | | | | | | | | | |
| ≧65 | 13 | 22 | 0.9684 | 4 | 31 | <0.9999 | 11 | 24 | 0.1588 |
| <65 | 11 | 19 | | 5 | 35 | | 7 | 33 | |
| Tumor size (cm) | | | | | | | | | |
| >3 | 11 | 27 | 0.7801 | 6 | 32 | 0.7223 | 7 | 31 | 0.5182 |
| ≦3 | 9 | 19 | | 3 | 25 | | 7 | 21 | |
| Unknown | 4 | 5 | | 0 | 9 | | 4 | 5 | |
| pT stage | | | | | | | | | |
| ≧pT2 | 12 | 14 | 0.0635 | 5 | 21 | 0.2632 | 9 | 17 | 0.1289 |
| ≦pT3 | 12 | 36 | | 4 | 44 | | 9 | 39 | |
| Unknown | 0 | 1 | | 0 | 1 | | 0 | 1 | |
| pN | | | | | | | | | |
| − | 19 | 35 | 0.343 | 8 | 46 | 0.4304 | 13 | 41 | 0.9999< |
| + | 5 | 16 | | 1 | 20 | | 5 | 16 | |
| CEA (ng/mL) | | | | | | | | | |
| ≧5 | 14 | 25 | 0.6158 | 5 | 34 | <0.9999 | 10 | 29 | 0.8914 |
| <5 | 10 | 23 | | 4 | 29 | | 8 | 25 | |
| Unknown | 0 | 3 | | 0 | 3 | | 0 | 3 | |
| Chemotherapy | | | | | | | | | |
| − | 8 | 23 | 0.3345 | 4 | 27 | <0.9999 | 4 | 27 | 0.098 |
| + | 16 | 28 | | 5 | 39 | | 14 | 30 | |
| Histological regression | | | | | | | | | |
| Low | 9 | 29 | 0.1578 | 3 | 35 | 0.3024 | 8 | 30 | 0.6866 |
| High | 14 | 22 | | 6 | 30 | | 9 | 27 | |
| Unknown | 1 | 0 | | 0 | 1 | | 1 | 0 | |
| Tumor downsizing | | | | | | | | | |
| Size ratio ≦0.6 | 14 | 21 | 0.0685 | 6 | 29 | 0.4837 | 10 | 25 | 0.1428 |
| Size ratio >0.6 | 6 | 25 | | 3 | 28 | | 4 | 27 | |
| Unknown | 4 | 5 | | 0 | 9 | | 4 | 5 | |

*pN* pathological lymph node metastasis

Bold faced values indicate $p$ values with statistical significance (i.e. values less than 0.05)

primary legions was more prominent and pathological T2 stage (indicating down-stage in the T stage) was more frequent; however, differences were not statistically significant.

Table 3 shows the clinical and pathological features, including the presence of these major adverse events (leukocytopenia and diarrhea), of the patients and the 5-year relapse-free survival rate. Patients with pathological T2 stage (85±8% vs. 48±10%, $p$=0.0076), those without pathological lymph node metastasis in the resected specimen (69±8% vs. 37±14%, $p$=0.0046), and those with leukocytopenia or diarrhea (94±5% vs. 49±9%, $p$=0.0054, Fig. 1) showed a significantly better 5-year relapse-free survival rate than their counterparts. Histological regression and tumor downsizing were not significantly associated with relapse-free survival. In the multivariate analysis, the presence of adverse events (leukocytopenia or diarrhea) was an independent predictor of better relapse-free survival, and the pathological T stage and lymph node metastasis lost their statistical significance as prognostic factors, as observed in the univariate analysis (Table 4).

**Table 3** Clinical and pathological features and 5-year disease-free survival

| | *n* | 5-year RFS[a] | *p* value |
|---|---|---|---|
| Sex | | | |
| Male | 57 (76%) | 64±36 | 0.9291 |
| Female | 18 (24%) | 60±12 | |
| Age (years) | | | |
| ≧65 | 35 (47%) | 69±31 | 0.6693 |
| <65 | 40 (53%) | 55±11 | |
| Tumor size (cm) | | | |
| >3 | 30 (40%) | 67±10 | 0.5048 |
| ≦3 | 42 (56%) | 64±12 | |
| Unknown | 3 (4%) | | |
| pT stage | | | |
| ≧pT2 | 26 (35%) | 85±8 | **0.0076** |
| ≦pT3 | 48 (64%) | 48±10 | |
| Unknown | 1 (1%) | | |
| pN | | | |
| − | 54 (72%) | 69±8 | **0.0046** |
| + | 21 (28%) | 37±14 | |
| CEA (ng/mL) | | | |
| ≧5 | 39 (52%) | 70±9 | 0.3731 |
| <5 | 33 (44%) | 55±11 | |
| Unknown | 3 (4%) | | |
| Chemotherapy | | | |
| − | 31 (41%) | 62±9 | 0.8928 |
| + | 44 (59%) | 65±10 | |
| Histological regression | | | |
| Low | 38 (51%) | 50±11 | 0.0838 |
| High | 36 (48%) | 80±8 | |
| Unknown | 1 (1%) | | |
| Tumor downsizing | | | |
| Size ratio ≦0.6 | 35 (47%) | 72±9 | 0.6018 |
| Size ratio >0.6 | 31 (41%) | 60±12 | |
| Unknown | 9 (12%) | | |
| Leukocytopenia/diarrhea | | | |
| − | 51 (68%) | 49±9 | **0.0054** |
| + | 24 (32%) | 94±5 | |

*RFS* relapse-free survival, *pN* pathological lymph node metastasis

[a] Values are expressed as survival rates±standard errors

Bold faced values indicate $p$ values with statistical significance (i.e. values less than 0.05)

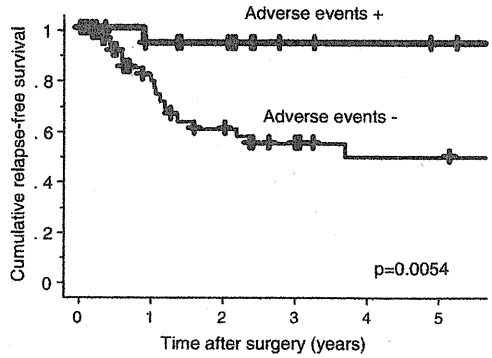


**Fig. 1** Relapse-free survival of the patients with and without leukocytopenia or diarrhea following preoperative radiotherapy. *Adverse events* leukocytopenia or diarrhea, *plus sign* censored patients

## Discussion

We found in this study that the rectal cancer patients who suffered from adverse events following PRT showed a better relapse-free survival than those who did not. Adverse events may occur following PRT for rectal cancers; however, severe ones are reported to be relatively infrequent, and the majority of the patients complete the planned course of neoadjuvant therapy [5–7]. The incidence of grade 3–4 toxicity is reported to be around 3–7% in radiotherapy alone, and 3–50% in chemoradiotherapy [5, 6, 11–13], which varies widely among literatures. The incidence of adverse events can be influenced by treatment factors, such as use of concomitant chemotherapy or not, chemotherapy regimen, and patient position during radiotherapy. In this study, the majority of the adverse event of PRT was grade 1–2 and all but three patients, who required reduction or discontinuation of chemotherapy, completed the planned PRT, which was in accordance with the reports of well-tolerated radiotherapy or chemoradiotherapy using tegafur-uracil and leucovorin, which were employed in this study [5, 13]. Tegafur-uracil is shown to improve patient survival when given as postoperative adjuvant chemotherapy for stage III rectal cancer [14] and is widely used for colorectal cancer in Japan. Our study showed a relatively mild toxic profile of tegafur-uracil and leucovorin when

**Table 4** Analysis of prognostic factors

| | *n* | Univariate analysis | | Multivariate analysis | |
|---|---|---|---|---|---|
| | | HR (95% CI) | *p* value | HR (95% CI) | *p* value |
| Sex | | | | | |
| Male | 57 | 1 | 0.9291 | | |
| Female | 18 | 1.044 (0.401–2.722) | | | |
| Age (years) | | | | | |
| ≧65 | 35 | 0.823 (0.335–2.018) | 0.6698 | | |
| <65 | 40 | 1 | | | |
| Tumor size (cm) | | | | | |
| >3 | 30 | 1 | 0.3885 | | |
| ≦3 | 42 | 1.508 (0.593–3.834) | | | |
| pT stage | | | | | |
| ≧pT2 | 26 | 0.217 (0.063–0.774) | **0.015** | 0.309 (0.088–1.089) | 0.0676 |
| ≦pT3 | 48 | 1 | | 1 | |
| pN | | | | | |
| − | 54 | 0.291 (0.118–0.720) | **0.0076** | 0.478 (0.190–1.205) | 0.1178 |
| + | 21 | 1 | | 1 | |
| CEA (ng/mL) | | | | | |
| ≧5 | 39 | 1 | 0.3763 | | |
| <5 | 33 | 1.502 (0.610–3.698) | | | |
| Chemotherapy | | | | | |
| − | 31 | 1 | 0.8289 | | |
| + | 44 | 0.940 (0.380–2.324) | | | |
| Histological regression | | | | | |
| Low | 38 | 1 | 0.0928 | | |
| High | 36 | 0.436 (0.166–1.148) | | | |
| Tumor downsizing | | | | | |
| Size ratio ≦0.6 | 35 | 1 | 0.6028 | | |
| Size ratio >0.6 | 31 | 1.300 (0.484–3.486) | | | |
| Leukocytopenia/diarrhea | | | | | |
| − | 51 | 1 | **0.0244** | 1 | **0.0494** |
| + | 24 | 0.099 (0.013–0.742) | | 0.132 (0.017–0.995) | |

*HR* hazard ratio, *CI* confidence interval, *pN* pathological lymph node metastasis

Bold faced values indicate *p* values with statistical significance (i.e. values less than 0.05)

administered with PRT. Patients treated with PRT with or without concomitant chemotherapy were analyzed together in this study because of a relatively small size of study population, and this is a limitation of this study. However, the presence of adverse events was a prognostic factor independent of the use of concomitant chemotherapy. Recently, the prone patient position with the belly board device is shown to reduce gastrointestinal toxicity of pelvic radiotherapy, especially of diarrhea, by reduction of the small bowel involvement in the radiation field [15]. In this study, radiotherapy was given in the supine position because of the problems in the treatment reproducibility of the prone position without belly board which we lack; however, no apparent increase of diarrhea was observed compared to the reported series of chemoradiotherapy given in the prone position [16, 17].

In contrast to the treatment factors that influence the incidence of adverse events, the individual patient factors that predispose patients toward PRT-related adverse events are largely unknown. In this study, female patients experienced leukocytopenia, not diarrhea, more frequently than male patients. In reports of 5-fluorouracil (5-FU)-based chemotherapy for colorectal cancers, female patients are shown to have higher risk for severe toxicity [18, 19]. It has been also reported that activity of dihydropyrimidine dehydrogenase (DPD), the initial enzyme in the catabolism of 5-FU, is lower in women compared with men [20], and possible association with its decreased activity in female patients and 5-FU-related toxicity is suggested [21]. In this study, the proportion of the patients receiving chemotherapy with radiotherapy was not different between the male and female patients (59.6% vs. 55.6%, respectively, $p$=0.7585); thus, decreased DPD activity might also have been involved in the presence of leukocytopenia in female patients receiving chemoradiotherapy. Other patient factors, such as race and dietary habit of the patients, might influence the toxicity of PRT; however, our study population comprised only Japanese, and the impact of them remains to be elucidated.

Although not statistically significant, the presence of leukocytopenia or diarrhea tended to be associated with pathological T2 stage or less, which was considered as down-staging, and high histological regression and down-sizing of the primary lesions. Patients who experienced leukocytopenia or diarrhea showed significantly better relapse-free survival than those who did not, and the presence of these adverse events represented an independent prognostic factor in the multivariate analysis. Thus, the therapeutic effect of PRT was suggested to be higher in the patients with these adverse events than in those without. Leukocytopenia and diarrhea caused by radiotherapy or chemotherapy are considered to be due to the toxic effect on the bone marrow and the intestinal mucosa; therefore, the presence of these adverse events might indicate the susceptibility of normal cells or tissues to radiotherapy or chemotherapy of the patient. In the literatures of chemotherapy for colorectal cancer, key enzymes involved in the metabolism of 5-FU, such as DPD and thymidylate synthase (TS), have been shown to be associated both with the efficacy and toxicity of 5-FU [19, 21–23], and in patients treated with cetuximab, the correlation between skin toxicity and response and/or survival is well documented [24, 25]. Therefore, toxicity and efficacy, that is, damage of normal cells and malignant cells in response to chemotherapy, are suggested to be regulated by the shared factors. In the same way, there might be some underlying factors, genetic or nongenetic, which contribute to both the toxicity and efficacy of PRT.

Pathological T stage and lymph node metastasis are well-documented prognostic factors of colorectal cancers [26, 27]. In this study, they are also significantly correlated with relapse-free survival in the univariate analysis and log-rank test. However, they did not show statistical significance when analyzed in the multivariate analysis together with the presence of adverse events. This might be because, in some patients, T stage is down-staged and lymph node metastasis, if present, is sterilized following PRT, and this therapeutic effect of PRT might make the prognostic significance of these factors less clear.

In conclusion, although a quarter of the patients experienced leukocytopenia or diarrhea following PRT, they were relatively mild and successfully controlled in the majority of the cases. Female patients experienced leukocytopenia more frequently than male patients; otherwise, no apparent predisposing factor for adverse events of PRT was recognized. The presence of leukocytopenia or diarrhea was an independent predictor of a fair prognosis after curative operation following PRT, and thus these adverse events seem not to discourage oncologists and patients from the indication of PRT for rectal cancers. Future prospective study of larger patient population is necessary to confirm our observations.

## References


1. Colorectal Cancer Collaborative Group (2001) Adjuvant radiotherapy for rectal cancer: a systematic overview of 8, 507 patients from 22 randomised trials. Lancet 358(9290):1291–1304. doi:10.1016/S0140-6736(01)06409-1
2. Folkesson J, Birgisson H, Pahlman L, Cedermark B, Glimelius B, Gunnarsson U (2005) Swedish rectal cancer trial: long lasting benefits from radiotherapy on survival and local recurrence rate. J Clin Oncol 23(24):5644–5650. doi:10.1200/JCO.2005.08.144
3. Peeters KC, Marijnen CA, Nagtegaal ID, Kranenbarg EK, Putter H, Wiggers T, Rutten H, Pahlman L, Glimelius B, Leer JW, van de Velde CJ (2007) The TME trial after a median follow-up of 6 years: increased local control but no survival benefit in irradiated patients with resectable rectal carcinoma. Ann Surg 246(5):693–701. doi:10.1097/01.sla.0000257358.56863.ce
4. Sauer R, Becker H, Hohenberger W, Rodel C, Wittekind C, Fietkau R, Martus P, Tschmelitsch J, Hager E, Hess CF, Karstens JH, Liersch T, Schmidberger H, Raab R (2004) Preoperative versus postoperative chemoradiotherapy for rectal cancer. N Engl J Med 351(17):1731–1740. doi:10.1056/NEJMoa040694
5. Gerard JP, Conroy T, Bonnetain F, Bouche O, Chapet O, Closon-Dejardin MT, Untereiner M, Leduc B, Francois E, Maurel J, Seitz JF, Buecher B, Mackiewicz R, Ducreux M, Bedenne L (2006) Preoperative radiotherapy with or without concurrent fluorouracil and leucovorin in T3–4 rectal cancers: results of ffcd 9203. J Clin Oncol 24(28):4620–4625. doi:10.1200/JCO.2006.06.7629
6. Bosset JF, Collette L, Calais G, Mineur L, Maingon P, Radosevic-Jelic L, Daban A, Bardet E, Beny A, Ollier JC (2006) Chemotherapy with preoperative radiotherapy in rectal cancer. N Engl J Med 355 (11):1114–1123. doi:10.1056/NEJMoa060829
7. Mohiuddin M, Winter K, Mitchell E, Hanna N, Yuen A, Nichols C, Shane R, Hayostek C, Willett C (2006) Randomized phase II study of neoadjuvant combined-modality chemoradiation for distal rectal cancer: Radiation Therapy Oncology Group Trial 0012. J Clin Oncol 24(4):650–655. doi:10.1200/JCO.2005.03.6095
8. Kiyomatsu T, Watanabe T, Muto T, Nagawa H (2007) The 4-portal technique decreases adverse effects in preoperative radiotherapy for advanced rectal cancer: comparison between the 2-portal and the 4-portal techniques. Am J Surg 194(4):542–548. doi:10.1016/j.amjsurg.2007.01.030
9. Sobin L, Wittekind C (eds) (2002) TNM classification of malignant tumours. Springer, New York
10. Japanese Society for Cancer of the Colon and Rectum (2006) General rules for clinical and pathological studies on cancer of the colon, rectum and anus, 7th edn. Kanehira-Syuppan, Tokyo (in Japanese)
11. Bujko K, Nowacki MP, Nasierowska-Guttmejer A, Michalski W, Bebenek M, Kryj M (2006) Long-term results of a randomized trial comparing preoperative short-course radiotherapy with preoperative conventionally fractionated chemoradiation for rectal cancer. Br J Surg 93(10):1215–1223. doi:10.1002/bjs.5506
12. Chau I, Brown G, Cunningham D, Tait D, Wotherspoon A, Norman AR, Tebbutt N, Hill M, Ross PJ, Massey A, Oates J (2006) Neoadjuvant capecitabine and oxaliplatin followed by synchronous chemoradiation and total mesorectal excision in magnetic resonance imaging-defined poor-risk rectal cancer. J Clin Oncol 24(4):668–674. doi:10.1200/JCO.2005.04.4875
13. Kundel Y, Brenner B, Symon Z, Oberman B, Sadezki S, Koller M, Catane R, Pfeffer R (2007) A phase II study of oral UFT and leucovorin concurrently with pelvic irradiation as neoadjuvant chemoradiation for rectal cancer. Anticancer Res 27(4C):2877–2880
14. Akasu T, Moriya Y, Ohashi Y, Yoshida S, Shirao K, Kodaira S (2006) Adjuvant chemotherapy with uracil-tegafur for pathological stage III rectal cancer after mesorectal excision with selective lateral

pelvic lymphadenectomy: a multicenter randomized controlled trial. Jpn J Clin Oncol 36(4):237–244. doi:10.1093/jjco/hyl014
15. Shanahan TG, Mehta MP, Bertelrud KL, Buchler DA, Frank LE, Gehring MA, Kubsad SS, Utrie PC, Kinsella TJ (1990) Minimization of small bowel volume within treatment fields utilizing customized "Belly boards". Int J Radiat Oncol Biol Phys 19(2):469–476. doi:0360-3016(90)90559-3
16. Feliu J, Calvilio J, Escribano A, de Castro J, Sanchez ME, Mata A, Espinosa E, Garcia Grande A, Mateo A, Gonzalez Baron M (2002) Neoadjuvant therapy of rectal carcinoma with UFT-leucovorin plus radiotherapy. Ann Oncol 13(5):730–736
17. Giralt J, Tabernero J, Navalpotro B, Capdevila J, Espin E, Casado E, Manes A, Landolfi S, Sanchez-Garcia JL, de Torres I, Armengol M (2008) Pre-operative chemoradiotherapy with UFT and leucovorin in patients with advanced rectal cancer: a phase II study. Radiother Oncol. doi:10.1016/j.radonc.2008.07.010
18. Sloan JA, Goldberg RM, Sargent DJ, Vargas-Chanes D, Nair S, Cha SS, Novotny PJ, Poon MA, O'Connell MJ, Loprinzi CL (2002) Women experience greater toxicity with fluorouracil-based chemotherapy for colorectal cancer. J Clin Oncol 20(6):1491–1498
19. Schwab M, Zanger UM, Marx C, Schaeffeler E, Klein K, Dippon J, Kerb R, Blievernicht J, Fischer J, Hofmann U, Bokemeyer C, Eichelbaum M (2008) Role of genetic and nongenetic factors for fluorouracil treatment-related severe toxicity: a prospective clinical trial by the German 5-FU Toxicity Study Group. J Clin Oncol 26(13):2131–2138. doi:10.1200/JCO.2006.10.4182
20. Etienne MC, Lagrange JL, Dassonville O, Fleming R, Thyss A, Renee N, Schneider M, Demard F, Milano G (1994) Population study of dihydropyrimidine dehydrogenase in cancer patients. J Clin Oncol 12(11):2248–2253
21. van Kuilenburg AB (2004) Dihydropyrimidine dehydrogenase and the efficacy and toxicity of 5-fluorouracil. Eur J Cancer 40 (7):939–950. doi:10.1016/j.ejca.2003.12.004
22. Lecomte T, Ferraz JM, Zinzindohoue F, Loriot MA, Tregouet DA, Landi B, Berger A, Cugnenc PH, Jian R, Beaune P, Laurent-Puig P (2004) Thymidylate synthase gene polymorphism predicts toxicity in colorectal cancer patients receiving 5-fluorouracil-based chemotherapy. Clin Cancer Res 10(17):5880–5888. doi:10.1158/1078-0432.CCR-04-0169
23. Ichikawa W, Uetake H, Shirota Y, Yamada H, Takahashi T, Nihei Z, Sugihara K, Sasaki Y, Hirayama R (2003) Both gene expression for orotate phosphoribosyltransferase and its ratio to dihydropyrimidine dehydrogenase influence outcome following fluoropyrimidine-based chemotherapy for metastatic colorectal cancer. Br J Cancer 89(8):1486–1492. doi:10.1038/sj.bjc.6601335
24. Racca P, Fanchini L, Caliendo V, Ritorto G, Evangelista W, Volpatto R, Milanesi E, Ciorba A, Paris M, Facilissimo I, Macripo G, Clerico M, Ciuffreda L (2008) Efficacy and skin toxicity management with cetuximab in metastatic colorectal cancer: outcomes from an oncologic/dermatologic cooperation. Clin Colorectal Cancer 7(1):48–54
25. Jonker DJ, O'Callaghan CJ, Karapetis CS, Zalcberg JR, Tu D, Au HJ, Berry SR, Krahn M, Price T, Simes RJ, Tebbutt NC, van Hazel G, Wierzbicki R, Langer C, Moore MJ (2007) Cetuximab for the treatment of colorectal cancer. N Engl J Med 357 (20):2040–2048. doi:10.1056/NEJMoa071834
26. Compton CC, Fielding LP, Burgart LJ, Conley B, Cooper HS, Hamilton SR, Hammond ME, Henson DE, Hutter RV, Nagle RB, Nielsen ML, Sargent DJ, Taylor CR, Welton M, Willett C (2000) Prognostic factors in colorectal cancer. College of American Pathologists Consensus Statement 1999. Arch Pathol Lab Med 124(7):979–994
27. Bujko K, Michalski W, Kepka L, Nowacki MP, Nasierowska-Guttmejer A, Tokar P, Dymecki D, Pawlak M, Lesniak T, Richter P, Wojnar A, Chmielik E (2007) Association between pathologic response in metastatic lymph nodes after preoperative chemoradiotherapy and risk of distant metastases in rectal cancer: an analysis of outcomes in a randomized trial. Int J Radiat Oncol Biol Phys 67(2):369–377. doi:10.1016/j.ijrobp.2006.08.065